Hindawi
Complexity
Volume 2022, Article ID 4155397, 17 pages
https://doi.org/10.1155/2022/4155397

Research Article

Regular and Chaotic Behavior on the Convection in a Rotating Ferrofluid in Porous Medium under Helical Force

M.L. Hounvènou and Vincent Adjimon Monwanou

Laboratoire de Mécaniques des Fluides, de La Dynamique Non-linéaire et de La Modélisation des Systèmes Biologiques (LMFDNMSB), Institut de Mathématiques et de Sciences Physiques (IMSP), Porto-Novo, Benin

Correspondence should be addressed to Vincent Adjimon Monwanou; vincent.monwanou@imsp-uac.org

Received 8 May 2022; Accepted 29 August 2022; Published 19 September 2022

Academic Editor: Saleh Mobayen

This article deals with the control of chaos on the convective motion in a ferrofluid filled in a rotating porous medium and under the helical force effect. We performed a truncated expansion of Galerkin and found the Lorenz-type model which described the system. The dynamical system is characterized using appropriate and subsequent criteria. We noticed that the system presents regular and chaotic behaviors according to the parameters at present. A considerable reduction of the chaotic domain is noticed with the increase of the intensity of the helical force and of the Darcy number, thus making it possible to delay the heat transfer in the system. The increase in the viscosity ratio and the Taylor number widen the chaotic domain leading to an acceleration of the heat transfer in the system.

1. Introduction

Since its discovery in the 20th century, chaos has been one of the most interesting for dynamic systems in areas such as physics, mathematics, chemistry, biochemistry, economics and finance, epidemiology, and engineering. [1–6]. Depending on the field of study, chaos is sometimes useful or undesirable to the point where many researchers are interested in its prediction and/or control. For example, in communications engineering, chaos allows to encode information or to encrypt images (synchronization and/or antisynchronization of chaotic systems) [7]. In the construction engineering of large infrastructures (the case of bridges for example), chaos is to be avoided. Naturally and this in almost all domains, the dynamic systems encountered are nonlinear. But the most important factors favoring chaos are nonlinearity and sensitivity to initial conditions, so nonlinear dynamic systems have a strong chance to develop chaotic behaviors followed by strong instabilities. Due to the complexity of these nonlinear dynamic systems, analytically process and finding exact solutions are often difficult. For this reason, several approximate analytical methods and numerical simulations are used.

The theory of ferrofluids has attracted attention of many researchers since their appearance, because their applications are numerous in various fields. Ferrofluids are also called magnetic fluids. They are composed of colloidal suspensions of nanosized ferromagnetic particles stably dispersed in organic or nonorganic carrier fluids which can be water, kerosene, and hydrocarbon. Due to their use in a variety of engineering applications, commercial production has been of a large quantity. Also, the heat transfer with magnetic fluids as the support has been one of the leading area of scientific study due to its technological applications.

Chaotic convection in fluid layer is very interesting due to its relevance in a wide range of industrial applications. In a three-dimensional phase space, chaos was obtained for the Lorenz system [8] arising from the truncation of the classical Rayleigh–Bénard convection model. In a fluid layer, chaotic behavior can be actually advantageous in various industrial applications such as the production of crystals, oil reservoir modeling, and catalytic packed bed filtration.

The study of chaos can generally be carried out in various fields of physics. For example, a complete analytical study on the bifurcations and chaotic phenomena raised in certain second-order, nonautonomous, dissipative chaotic systems is reported by the author of [9].

Singh et al. [10] studied feedback control of chaotic convection in a porous medium under gravity modulation. They obtained a nonautonomous system with three differential equations by employing the truncated Galerkin expansion method in the modulated momentum and energy equations. The control with the Rayleigh number demonstrates either periodic or chaotic behavior of the system. The influence of the modulated amplitude is also found to advance the chaotic nature of the system whereas the feedback control and frequency of modulation parameters delay the chaotic behavior.

Control of chaos in a thermal convection loop by state space linearization has been investigated by Rana et al. [11]. A laminar flow has been obtained from a chaotic flow of the thermal convection loop by applying a technique state space linearization converting the nonlinear system into the linear system through a coordinate transformation, based on the concept of Lie brackets.

Ahmed et al. [12] studied natural convection flows of an incompressible Newtonian fluid filled in a circular cylinder and described the heat transfer process by a generalized fractional constitutive equation for the thermal flux-temperature gradient. They obtained the analytical solutions to the fluid temperature, thermal flux, fluid velocity, and volume flow rate using Laplace transform and finite Hankel transform.

Izadi et al. [13] treated computational analysis of thermal gravitational convection within a porous chamber under the impact of tilted periodic magnetic force and used Galerkin finite element method to resolve governing equations found from the study. They then have examined the impacts of the Darcy number, Hartmann number, Rayleigh number, periodicity of the magnetic field, magnetic field inclination angle, thermal conductivity ratio, and medium porosity on flow and thermal patterns. The study pointed out that parameters of the periodic magnetic field have the nonmonotonic influence of the heat transfer performance.

Convective chaos in fluids has received particular attention in recent years. Many works of chaotic convection have been done before with various additional effects in a different type of fluid due to its importance. Indeed, it makes it possible to highlight heat exchanges for large applications in the laboratory and in engineering. The case of magnetic fluid, due to its technological applications, has attracted the attention of several researchers. The chaos control on convection in fluids was carried out with the use of different types of fluid from simple fluid to magnetic one and in porous and nonporous media [14–23].

Laroze et al. [24] studied before theoretically and numerically the thermal convection in a magnetic suspension and modeled magnetic properties as those of electrically nonconducting superparamagnets by performing a truncated Galerkin expansion. Based on bifurcation diagrams, and Lyapunov exponents, they found that the system exhibits multiple transitions according to the parameters at present. The convection dynamics was studied in viscoelastic fluid in a porous medium [16] where the authors applied truncated expansion of Galerkin and obtained a generalized four-dimensional Lorenz system. Using the appropriate bifurcation curves and their corresponding Lyapunov exponents, they characterized the nonlinear dynamics of the system and found within a range of moderate and high Rayleigh numbers the proportional controller gain to enhance the stabilization and destabilization effects on the thermal convection. The system also exhibits remarkable topological structures.

Chaotic convection was carried out in a viscoelastic fluid with various technics and considerations as well as the stability analysis and has given very varied and very interesting results [25–37].

In a convective system, the pseudo-vector nature force responsible for helical turbulence is helical force. Hounvenou and Monwanou [19], in a recent work, studied the action of this force on chaotic convection in a magnetic fluid and come to the conclusion that this force reduces the chaotic domain.

Summarizing the literature, it comes that only the effect of rotation has been studied on the chaotic convection of a magnetic fluid in one case, then only the effect of porosity in another case. The combined effect of the three effects on the chaotic convection of a magnetic fluid has not been studied because of the difficulties that this could cause. Overcoming all these difficulties would therefore be a major scientific challenge. So, in our work, we have decided to study the effect of this pseudo-vector type force on the chaotic convection in a rotating porous medium filled by a magnetic fluid. This study can reveal useful behaviors for its application in the field of technology and engineering.

We derive a set of nonlinear differential equations for the magnitudes of flow rate, temperature, magnetic particle concentration, and magnetic potential using a truncated Galerkin expansion. The dynamic behavior of the system has been characterized by plotting bifurcation diagrams, Lyapunov exponents, and phase diagrams which show chaotic and periodic behaviors.

The paper is organized as follows: in section 2, the basic equations for the convection in a rotating porous medium filled by a magnetic fluid and subject to the helical force are presented. Section 3 deals with the deriving of Lorenz-type equations using a truncated expansion of Galerkin. In section 4, the analysis of the stability of the solutions is made. Numerical simulations are performed, and the results are explained and discussed concerning the chaotic behavior in section 5. Finally, a conclusion is presented in the last section.

2. Basic Equations

We consider a porous rotating horizontal layer of thickness d of incompressible binary magnetic fluid subject to the effect of helical force. The configuration of the problem is illustrated in Figure 1.

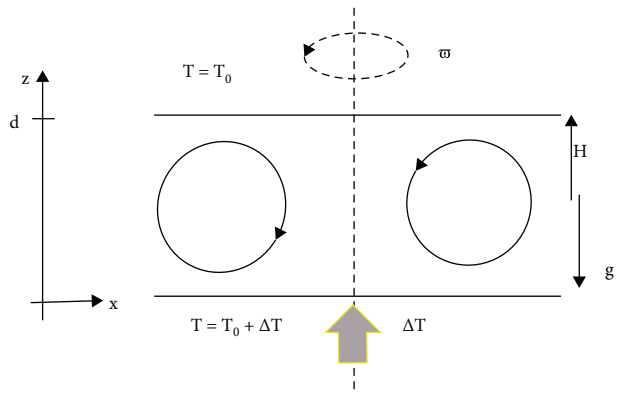

Figure 1: Problem configuration.

With the Boussinesq approximation, the equations describing the evolution of the binary ferrofluid under effect of helical force within the rotating porous medium in dimensionless form are written [38, 39] as

$$\nabla \cdot \mathbf{u} = 0, \tag{1}$$

$$\varepsilon^{-1}P^{-1}\left[\partial_t + \varepsilon^{-1}(\mathbf{u}.\nabla)\right]\mathbf{u} = -\nabla P_{\text{eff}} + \Lambda\nabla^2\mathbf{u} + Ra\Sigma + s\mathbf{f} + \text{Ta}^{1/2}(\mathbf{u}\wedge\mathbf{e}_z) - \text{Da}^{-1}\mathbf{u}, \tag{2}$$

$$d_t(\theta - M_4\partial_z\phi) = (1 - M_4)w + \nabla^2\theta + F\nabla^2(C - M_2\partial_z\phi), \tag{3}$$

$$d_tC = L\nabla^2(C + \theta - M_2\partial_z\phi), \tag{4}$$

$$\left(\partial_z^2 + M_3\nabla_\perp^2\right)\phi = \partial_z(\theta - \psi_m C), \tag{5}$$

$$\nabla^2_{\phi_{ext}} = 0, \tag{6}$$

where $\{\mathbf{u}, \theta, \phi\}$ are, respectively, the dimensionless perturbations of velocity, temperature, magnetic particle concentration, and magnetic potential.

$d_tf = \partial_t f + \mathbf{u}\cdot\nabla f$ is the particular derivative. P_{eff} is the effective pressure. Also, $\Sigma = \Pi_1(\theta, C, \phi)\widehat{z} - M_1(\theta - \psi_m C)\nabla(\partial_z\phi)$ with $\Pi_1(\theta, C, \phi) = (1 + M_1)\theta - (\psi + M_1\psi_m)C$ and $\nabla_\perp^2 = \partial_x^2 + \partial_y^2$.

The following dimensionless numbers appear in the equations (1)–(5):

Rayleigh number: $Ra = \alpha_T\rho_o g\beta d^4/\kappa\mu$

Prandtl number: $P = \mu/\rho_o\kappa$,

Darcy number: $Da = k_p/d^2$,

Brinkman number: $\Lambda = \mu_e/\mu$,

Intensity s of the helical force f: $s = a\varpi\varepsilon^{-1}d^2/\mu$.

Magnetic numbers are as follows:

$$M_1 = \frac{\beta\chi_T^2H_o^2}{[\rho_o g\alpha_T(1+\chi)]},$$

$$M_2 = \frac{\tilde{D}\chi_c\chi_T H_o^2}{[\rho_o\overline{D}_T(1+\chi)]},$$

$$M_3 = \frac{\left(1 + \chi_o + \chi_H H_o^2\right)}{(1+\chi)}, \tag{7}$$

$$M_4 = \frac{\chi_T H_o^2 T_o}{C_H(1+\chi)},$$

$$M_5 = \frac{\alpha_H\chi_T H_o^2}{\alpha_T(1+\chi)},$$

and $\psi_m = -\chi_c D_s/\chi_T D_c$.

Lewis number: $L = D_c/\kappa$,

Separation report: $\psi = \rho_o\overline{D}_T\alpha_c/\alpha_T\tilde{D}\gamma_H$, Dufour number: $F = \overline{D}_T^2/\tilde{D}\kappa$.

And, Taylor number: $Ta = (2\rho_o\varepsilon^{-1}\varpi d^2/\mu)^2$ with $D_c = \tilde{D}\gamma_H/\rho_o^2$ and $D_s = \overline{D}_T/\rho_o$.

The magnetic numbers used have the following orders of magnitude: $M_1 = 10^{-4} - 10$, $M_3 \simeq 1.1$, $M_4 \simeq M_5 \simeq 10^{-6}$ [24].

The values of the numbers M_4, M_5, and F are very small. This is why they will be neglected in the following calculations.

We express the velocity field as (the analysis is limited to a flow in dimension 2):

$\mathbf{u} = \{-\partial_z\Psi, 0, \partial_x\Psi\}$. Eliminating the pressure and the vorticity in equations (2)–(5), we obtain

$$\left[\left(\varepsilon^{-1}P^{-1}\partial_t - \Lambda\nabla_+^2 + Da^{-1}\right)^2\nabla_+^2 - s^2\left(\partial_x^2 - \partial_z^2\right)\partial_z^2 + Ta\partial_z^2 + Ta^{1/2}s\left[\partial_z^3 - \left(\partial_x^2 - \partial_z^2\right)\partial_z\right]\right]\partial_z\Psi = Ra\left(\varepsilon^{-1}P^{-1}\partial_t - \Lambda\nabla_+^2 + Da^{-1}\right)\partial_x^2\Xi, \tag{8}$$

$$d_t\theta = \partial_x\Psi + \nabla_+^2\theta, \tag{9}$$

$$d_tC = L\nabla_+^2(C + \theta - M_2\partial_z\phi), \tag{10}$$

$$\left(\partial_z^2 + M_3\partial_x^2\right)\phi = \partial_z(\theta - \psi_m C), \tag{11}$$

$$d_tf = \partial_t f + [\partial_x\Psi][\partial_z f] - [\partial_z\Psi][\partial_x f], \tag{12}$$

$\Xi = (1 + M_1)\theta - (\psi + M_1\psi_m)C = M_1\partial_z\phi$ and. $\nabla_+^2 f = \partial_x^2 f + \partial_z^2 f$.

We impose ideal boundary conditions $\theta = C = \Psi = \partial_z^2\Psi = \partial_z\phi = 0$ at $z = (0, 1)$ for temperature, magnetic particle concentration, and scalar magnetic potential stream function in order to solve equations (8)–(11) using the Galerkin method.

3. Galerkin Truncated Extension

We will restrict ourselves to the fundamental mode for the numerical simulations in the lateral direction since we consider a large container. In the z-direction across the layer, a multimode description will be used where necessary. Higher harmonics describe deviations of the variables from the linear regime [24]. According to the boundary conditions, we can represent the stream function, the temperature, and the concentration of the magnetic particles and the magnetic potential on the form below in order to obtain the solution of (8)–(11):

$$k\Psi(t, z, x) = a_1(t)\sin(\pi z)\sin(kx), \tag{13}$$

$$\theta(t, z, x) = a_2(t)\sin(\pi z)\cos(kx) + a_3(t)\sin(2\pi z), \tag{14}$$

$$C(t, z, x) = a_4(t)\sin(\pi z)\cos(kx) + a_5(t)\sin(2\pi z), \tag{15}$$

$$\phi(t, z, x) = a_6(t)\cos(\pi z)\cos(kx) + a_7(t)\cos(2\pi z), \tag{16}$$

with

$$a_6(t) = -\frac{\pi a_2(t)}{\pi^2 + k^2 M_3} \text{ and } a_7(t) = -\frac{a_3(t)}{2\pi}. \tag{17}$$

As in the Lorenz model, we only consider the temperature, the concentration, and consequently the scalar magnetic potential, the effect of the second harmonics. We have neglected the second harmonic of the current function due to the assumption of small convective motions [8].

Calculating the terms of the equations (8)–(11) with the Galerkin functions defined from (12)–(15), then multiplying the equations by the orthogonal eigenfunctions, and integrating them in space over the wavelength of a convection cell, $\int_{-\pi/k}^{\pi/k}\int_0^1\int_0^1 \mathrm{d}x\mathrm{d}z$, a set of ordinary differential equations is obtained for the temporal evolution of the amplitudes:

$$\begin{aligned}
\ddot{a}_1(t) = {} & -2\varepsilon P\left(\Lambda q^2 + Da^{-1}\right)\dot{a}_1 + \left[r\varepsilon P q^4 - \varepsilon^2 P^2\left[\Lambda^2 q^4 + Da^{-2} + \Lambda Da^{-1}\left(1 + q^2\right)\right] - \frac{\pi^2\varepsilon^2 P^2}{q^2}\left[Ta + \left(k^2 - \pi^2\right)s^2\right]\right]a_1(t) \\
& + \pi r\varepsilon P q^4 a_1(t)a_3(t) - \frac{\pi R a k^2 P}{q^2}\left(\psi + M_1\psi_m\right)a_1(t)a_5(t) \\
& + \left[rPq^6 - r\varepsilon^2 P^2\left(\Lambda q^2 + Da^{-1}\right)q^4 + \sigma R a k^2 P\left(\psi + M_1\psi_m\right)\right]a_1(t) \\
& + \frac{\varepsilon^2 P^2 k^2 R a}{q^2}\left(\psi + M_1\psi_m\right)\left(\Lambda q^2 + Da^{-1} - \varepsilon^{-1}P^{-1}q^2 L\right)a_4(t),
\end{aligned} \tag{18}$$

$$\dot{a}_2(t) = -a_1(t) - q^2 a_2(t) - \pi a_1(t)a_3(t),$$

$$\dot{a}_3(t) = -\frac{\pi}{2}a_1(t)a_2(t) - 4\pi^2 a_3(t),$$

$$\dot{a}_4(t) = -\pi a_1(t)a_5(t) - Lq^2 a_4(t) + \sigma q^2 a_2(t),$$

$$a_5(t) = \frac{\pi}{2}a_1(t)a_4(t) - 4\pi^2 L a_5(t) - 4\pi^2 L\left(1 - M_2\right)a_3(t).$$

$q^2 = (k^2 + \pi^2), r = Ra/Ra_s$ and

$$\sigma = \frac{LM_2\pi^2 - L\left(\pi^2 + k^2 M_3\right)}{\pi^2 + k^2 M_3}. \tag{19}$$

r is the reduced number of Rayleigh [24]; Ra_s is the stationary Rayleigh number in the case of linear stability when $\psi = 0$ and $\psi_m = 0$ (Finlayson [40]).

$$Ra_s = \frac{q^6\left(\pi^2 + k^2 M_3\right)}{k^2\left[\pi^2 + k^2\left(1 + M_1\right)M_3\right]}. \tag{20}$$

4. Stability Analysis of the System

We use [19] and we set

$\tau = q^2 t$ and new variables $X(\tau) = \pi/q^2\sqrt{2}a_1(\tau)$, $Y(\tau) = \pi r/\sqrt{2} - a_2(\tau)$, $Z(\tau) = -\pi r a_3(\tau)$, $R(\tau) = -\pi r/\sqrt{2}a_4(\tau)$, and $S(\tau) = -\pi r a_5(\tau)$.

We get

$$\dot{X}(\tau) = W(\tau), \tag{21}$$

$$\dot{Y}(\tau) = rX(\tau) - Y(\tau) - X(\tau)Z(\tau), \tag{22}$$

$$\dot{Z}(\tau) = X(\tau)Y(\tau) - \eta Z(\tau), \tag{23}$$

$$\dot{R}(\tau) = -LR(\tau) + \sigma Y(\tau) - X(\tau)S(\tau), \tag{24}$$

$$\dot{S}(\tau) = -\eta LS(\tau) + X(\tau)R(\tau) - \eta L(1 - M_2)Z(\tau), \tag{25}$$

$$\begin{aligned}\dot{W}(\tau) = &-2\varepsilon P\left(\Lambda + \frac{2}{3\pi^2}Da^{-1}\right)W(\tau) - \varepsilon PX(\tau)Z(\tau)\\ &+ \varepsilon P\left[\varepsilon P\left(\Lambda + \frac{2}{3\pi^2}Da^{-1}\right) - 1\right]Y(\tau)\\ &+ \varepsilon P\left[r - \varepsilon P\left[\left(\frac{4}{9\pi^2} + \frac{2}{3\pi^2}\right)\Lambda Da^{-1} + \Lambda^2 + \frac{4}{27\pi^4}Ta - \frac{4}{27\pi^2}s^2 + \frac{4}{9\pi^2}Da^{-2}\right]\right]X(\tau).\end{aligned} \tag{26}$$

with $\eta = 4\pi^2/q^2$ and $\dot{f}(\tau) = \mathrm{d}f(\tau)/d\tau$.

We recover existing results in literature from the above formula. When $C \longrightarrow 0$, $M_1 = 0$ or $M_3 = 0\,(Q_{13} = 0)$, and $q^2 \longrightarrow 3\pi^2/2$, we retrieve Lorenz's system [8]. When $C = 0, Ta = 0$, and $s = 0$, the Lorenz system obtained by Laroze [24] is recovered.

If $s \longrightarrow 0$, $Da^{-1} \approx 0, \Lambda \longrightarrow 1$, and $\varepsilon \longrightarrow 1$, we recover the system studied in [28].

4.1. Dissipation Effect

$$\nabla V = \frac{\partial \dot{X}}{\partial X} + \frac{\partial \dot{Y}}{\partial Y} + \frac{\partial \dot{Z}}{\partial Z} + \frac{\partial \dot{R}}{\partial R} + \frac{\partial \dot{S}}{\partial S} + \frac{\partial \dot{W}}{\partial W} = -\eta(1 + L) - \left(1 + L + 2\varepsilon P\left(\Lambda + \frac{2}{3\pi^2}Da^{-1}\right)\right) < 0. \tag{27}$$

The system (21)–(26) is then dissipative. Therefore, the endpoints of the trajectories of a set of initial points in phase space, which occupies the region $V(0)$ at time $t = 0$, will decrease in volume after some time t such that

$$V(t) = V(0)\exp\left[-\eta(1 + L) - \left(1 + L + 2\varepsilon P\left(\Lambda + \frac{2}{3\pi^2}Da^{-1}\right)\right)t\right]. \tag{28}$$

The volume then decreases exponentially over time.

4.2. Study of the Equilibrium Points. The system (21)–(26) has the form $\dot{X} = f(X)$, and the fixed points X_S are given by $f(X_S)$. The trivial equilibrium point E_1 is

$$(X_1, Y_1, Z_1, R_1, S_1, W_1) = (0, 0, 0, 0, 0, 0). \tag{29}$$

4.3. Analysis of the System Stability at the Trivial Equilibrium Points. The matrix associated with the dynamic system studied is as follows due to the stability conditions:

$$J(E_1) = \begin{pmatrix} 0 & 0 & 0 & 0 & 0 & 1\\ r & -1 & 0 & 0 & 0 & 0\\ 0 & 0 & -\eta & 0 & 0 & 0\\ 0 & \sigma & 0 & -L & 0 & 0\\ 0 & 0 & -\eta mL & 0 & -\eta L & 0\\ Y & \zeta & 0 & 0 & 0 & -\beta \end{pmatrix} \tag{30}$$

with

$$\begin{aligned}\Upsilon &= \varepsilon P\left[r - \varepsilon P\left[\left(\frac{4}{9\pi^2} + \frac{2}{3\pi^2}\right)\Lambda Da^{-1} + \Lambda^2 + \frac{4}{27\pi^4}Ta - \frac{4}{27\pi^2}s^2 + \frac{4}{9\pi^2}Da^{-2}\right]\right],\\ \zeta &= \varepsilon P\left[\varepsilon P\left(\Lambda + \frac{2}{3\pi^2}Da^{-1}\right) - 1\right],\\ \beta &= -2\varepsilon P\left(\Lambda + \frac{2}{3\pi^2}Da^{-1}\right).\end{aligned} \tag{31}$$

The trivial fixed point polynomial characteristic equation is

$$P(\lambda) \equiv b_0\lambda^6 + b_1\lambda^5 + b_2\lambda^4 + b_3\lambda^3 + b_4\lambda^2 + b_5\lambda + b_6, \tag{32}$$

with

$$\begin{aligned}
b_0 &= 1,\\
b_1 &= (\eta + L + \eta L) + (1 + \beta),\\
b_2 &= \eta\left(1 + L^2\right) + (1 + \eta)[L(1 + \eta + \beta(1 + L)] - Y,\\
b_3 &= (1 + \eta)(\eta L\beta + \beta\eta)L + \eta L(1 + \eta + \beta L) + \beta\eta - [(1 + \eta)(1 + L) + \eta]Y,\\
b_4 &= \eta^2L^2 + \beta\eta L(1 + \eta)(1 + L) - [(1 + \eta)(1 + L) + \eta]Y,\\
b_5 &= \beta\eta^2L^2 - \left[\eta L + \eta L^2(1 + \eta)\right]Y,\\
b_6 &= -\eta^2L^2Y.
\end{aligned} \tag{33}$$

To determine the eigenvalues λ_i, we use the Routh–Hurwitz criterion [19, 41, 42].

Whatever $r > 0$, all the coefficients of the polynomial $P(\lambda)$ are positive. For < 1.1, the Hurwitz determinants verify $\Delta_{n-1} > 0, \Delta_{n-3} > 0$ for $\Lambda = 1, Da^{-1} \approx 0, s = 0$, and $Ta = 0$. The trivial fixed point is then stable for $r < 1.1$ when $\Lambda = 1, Da^{-1} \approx 0, s = 0$, and $Ta = 0$, and unstable otherwise. The fixed point E_1 is linearly unstable when the critical value of r is $r_c = 1.1$.

4.4. Regular and Chaotic Behavior Analysis. Numerical simulations are carried out in order to examine the effects of viscosity ratio Λ, the number of Darcy Da characteristic of the porosity of the medium, the helical force s, and the Taylor number Ta on the chaotic convection of the magnetic fluid. The fourth-order Runge-Kutta method is employed to solve numerically (21)–(26). We set the values $P = 10$, $\eta = 8/3$, $L = 1$, $M_2 = 1$, and $\sigma = -1/3$. The initial conditions are $X(0) = Y(0) = R(0) = W(0) = 0.8$ and $Z(0) = S(0) = 0.92195$.

We controlled the system formed by equations (21)–(26) with the reduced Rayleigh number r and the parameters above in presence.

In order to appreciate the effects of the parameters in presence on the system, we realize the bifurcation diagrams and their corresponding Lyapunov exponents, the phase portraits, and time stories.

The system has the possibility of having regular and chaotic behaviors according to the range of values to reduce Rayleigh number r (Figures 2–19).

Figures 2 and 3 show that at a certain increase in the viscosity ratio, with the fixed reduced Rayleigh number, the system is completely chaotic after a linear, an oscillatory, and two small periodic sequences, i.e., the heat transfer is progressively accelerated. The increase in the viscosity ratio makes the system completely chaotic.

Figure 4 shows that the system is linearly stable for $r = 1.56$, oscillatory for $46.95 \le r \le 58.125$, chaotic for $58.237764359 \le r \le 549.828$, $556.575 \le r \le 559.375$, and $r \ge 668, 754$, and periodic for $551.978 \le r \le 555.979$ and $661.505 \le r \le 668.251$.

Figures 5 and 6 show a reduction in the chaotic domain with the helical force. For a certain fixed value of r (Figure 6), for example, for $r = 670$ when the other parameters are kept fixed, the system is chaotic for $s = 0$ and $s = 2$ then periodic thereafter. We then conclude that for a value of the reduced number of Rayleigh r fixed, the system changes state, and the chaos slowly disappears when s increases, leaving the system in a periodic state of decreasing period. It can therefore be deduced that the increase in the helical force leads to a reduction of the chaotic domain of the system, corresponding to a delay of the heat transfer.

The system is linearly stable for $r = 1.447$, oscillatory for $25.899 \le r \le 35.6994$, chaotic for $37.83909 \le r \le 384.086$ and $429.00251 \le r \le 680.86$, and then periodic for $386.237 \le r \le 424, 946$ and $r \ge 683, 6$ (Figure 7).

Figures 8 and 9 show a reduction in the chaotic domain with the Darcy number leaving the system in a periodic state. Considering Figure 9, we notice that for a certain fixed value of r, for example, for $r = 362$, when the other parameters are kept fixed, the system is chaotic for Da = 0.09 then periodic: of period 2 for Da = 0.5 and of period 1 for Da = 1. It can be therefore concluded that the Darcy number Da reduces the chaotic domain of the system; i.e., the heat transfer is gradually retarded.

The system is linearly stable for $r = 1.45$, oscillatory for $25.59 \le r \le 35.6994$, chaotic for $36.9094 \le r \le 362.581$ and $403.441 \le r \le 637.849$, and then periodic for $364.731 \le r \le 399.14$ and $r \ge 640$ (Figure 10).

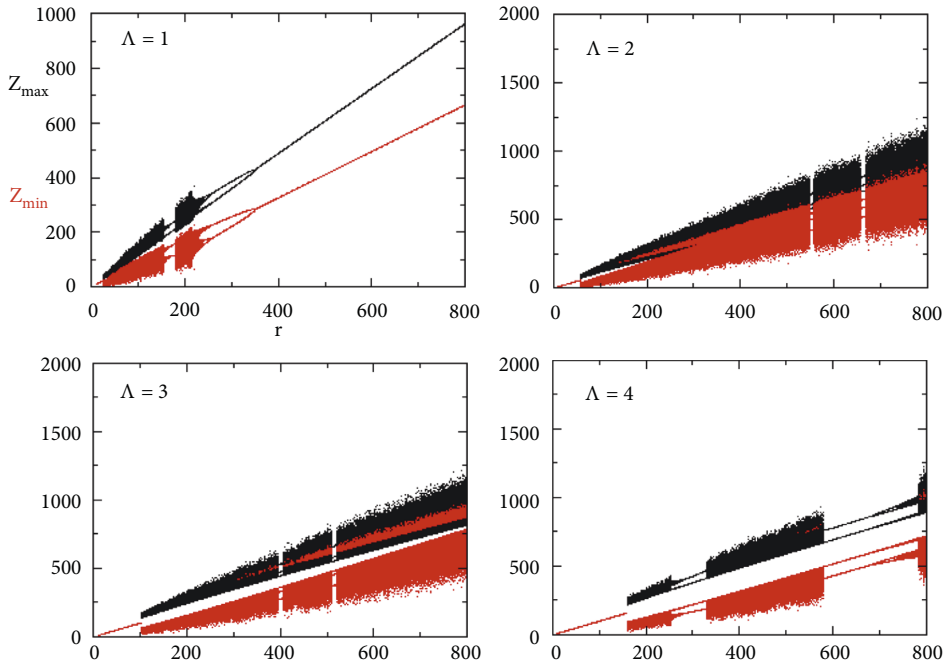

Figure 2: Diagrams of bifurcations of Z as a function of r representing the maxima and minima of the posttransient solution of $Z(\tau)$ showing the effect of the viscosity ratio Λ on the chaos of the system for $Da = 1$, $s = 0$, and $\mathrm{Ta} = 0$ with $P = 10$, $L = M_2 = 1$,$\eta = 8/3$, $k = \pi/\sqrt{2}$, $\varepsilon = 1$, and $\sigma = -1/3$.

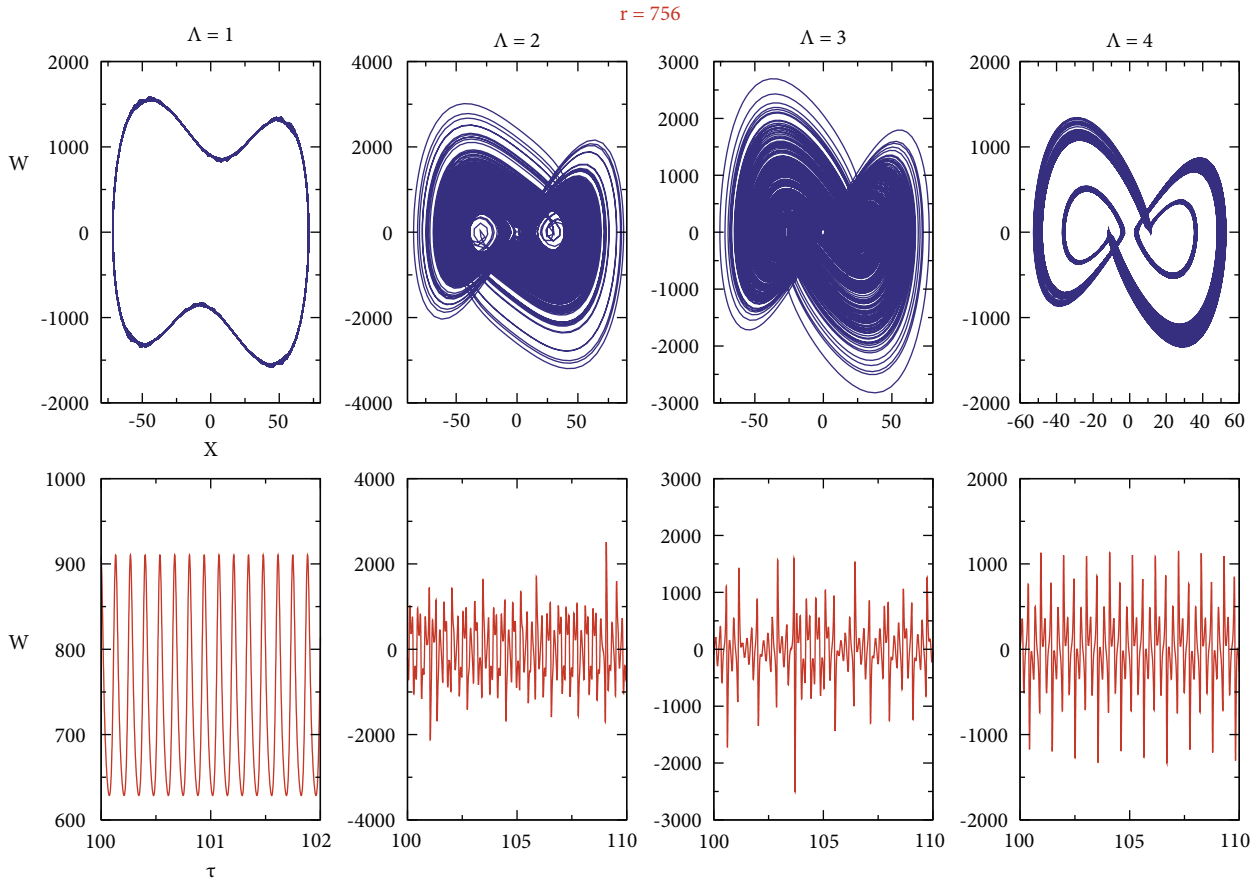

Figure 3: Phase portraits and time diagrams of the system for a fixed reduced Rayleigh number $r = 765$ and different values of Λ with the parameter values of Figure 2.

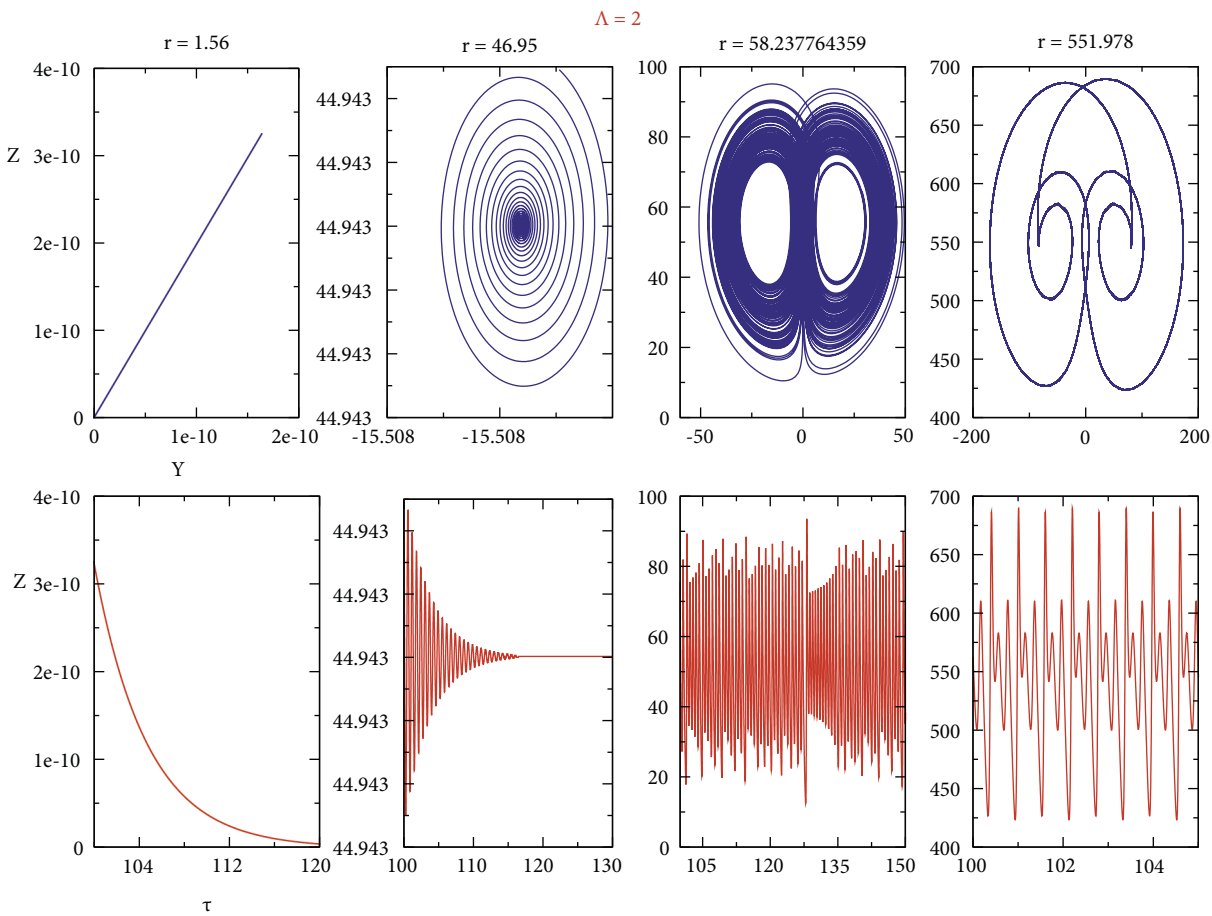

Figure 4: Phase portraits and time diagrams for different values of the reduced Rayleigh number r when $\Lambda = 2$ with the parameter values of Figure 2.

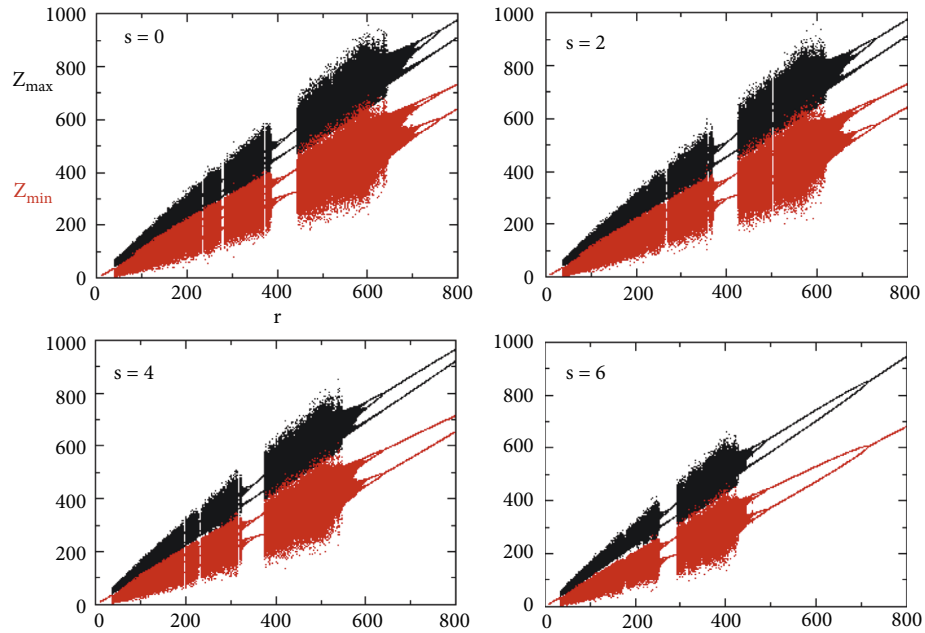

Figure 5: Diagrams of bifurcations of Z as a function of r showing the effect of the helical force on the chaos domain of the system when $\Lambda = 1Da = 0.09$, $Ta = 0$, $P = 10$, $L = M_2 = 1$,$\eta = 8/3$, $k = \pi/\sqrt{2}$, $\varepsilon = 1$, and$\sigma = -1/3$.

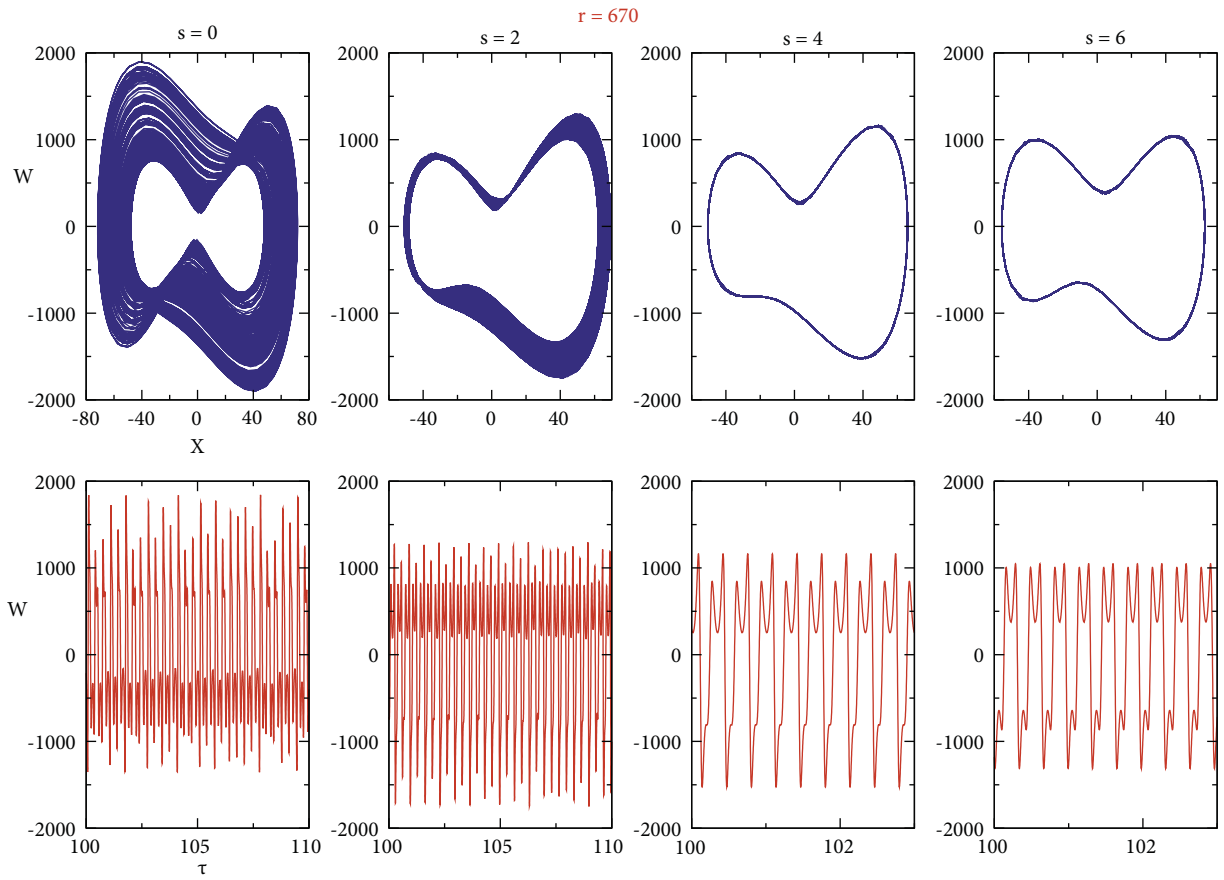

FIGURE 6: Phase portraits and time stories of the system for a fixed reduced Rayleigh number $r = 670$ and different values of s with the parameter values of Figure 5.

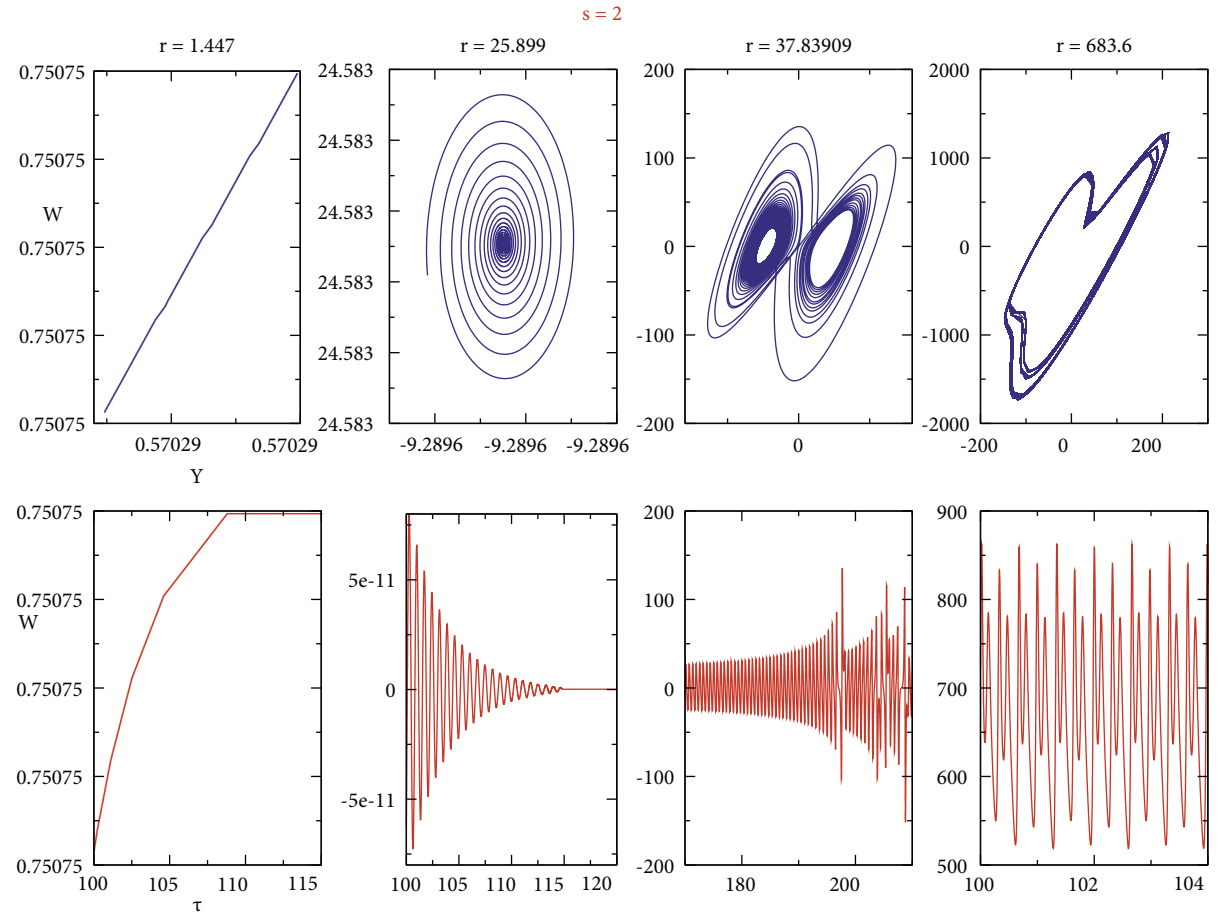

FIGURE 7: Phase portraits and time stories for different values of the reduced number of Rayleigh r when $s = 2$ with the parameter values of Figure 5.

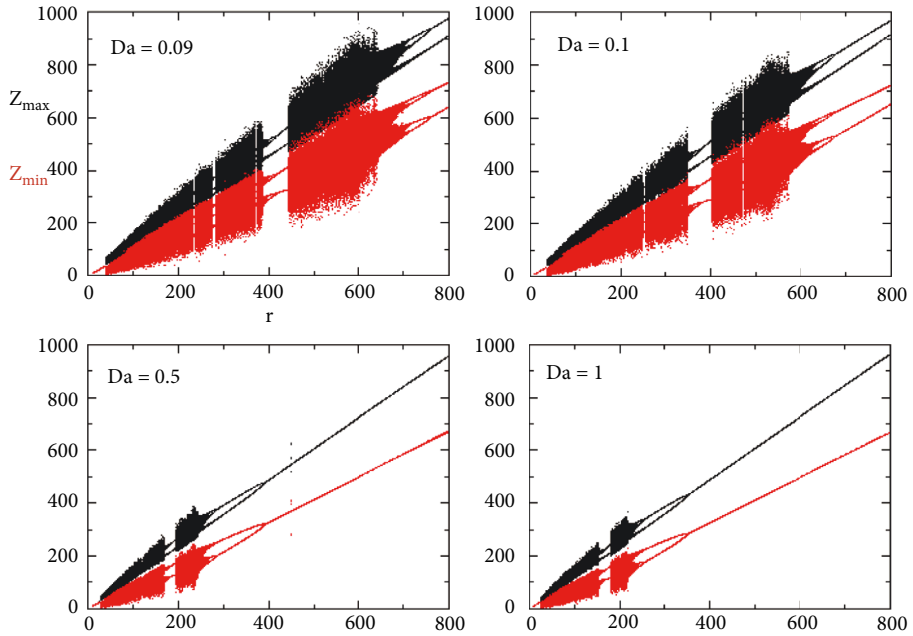

Figure 8: Diagrams of bifurcations of Z as a function of r showing the effect of the Darcy number Da on the chaos of the system when $s = 0$ with the parameter values of Figure 5.

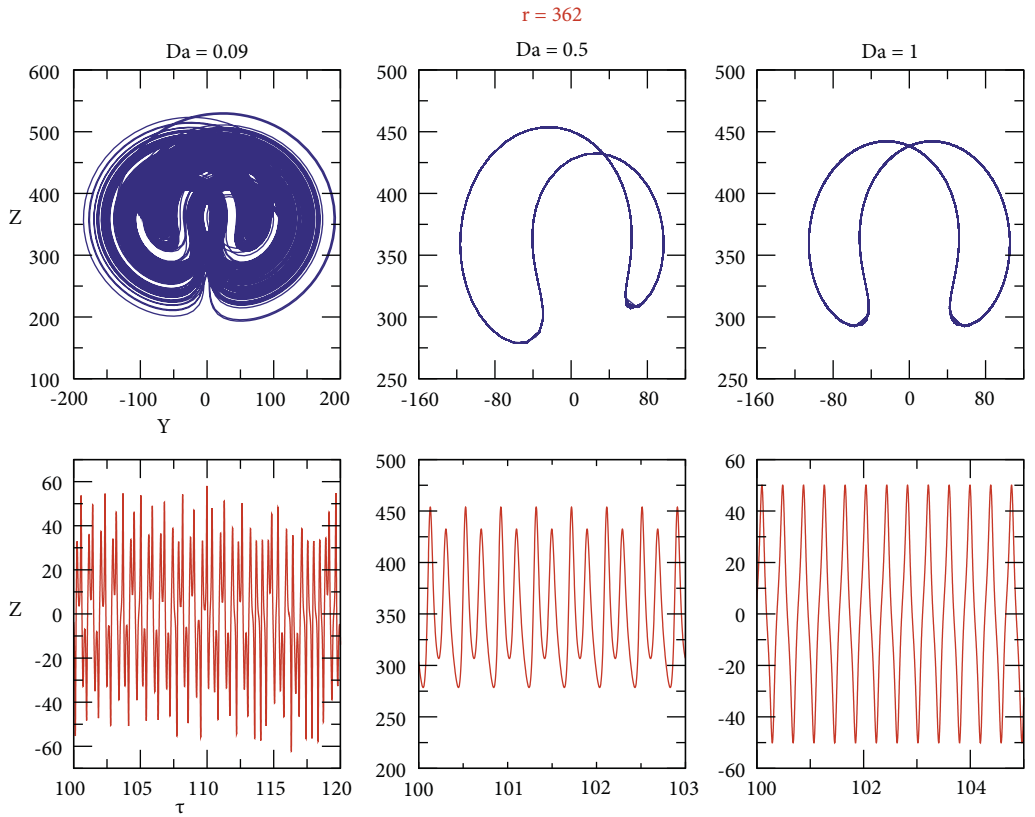

Figure 9: Phase portraits and time stories of the system for a fixed reduced number of Rayleigh $r = 362$ and different values of Da when $s = 0$ with the parameter values of Figure 5.

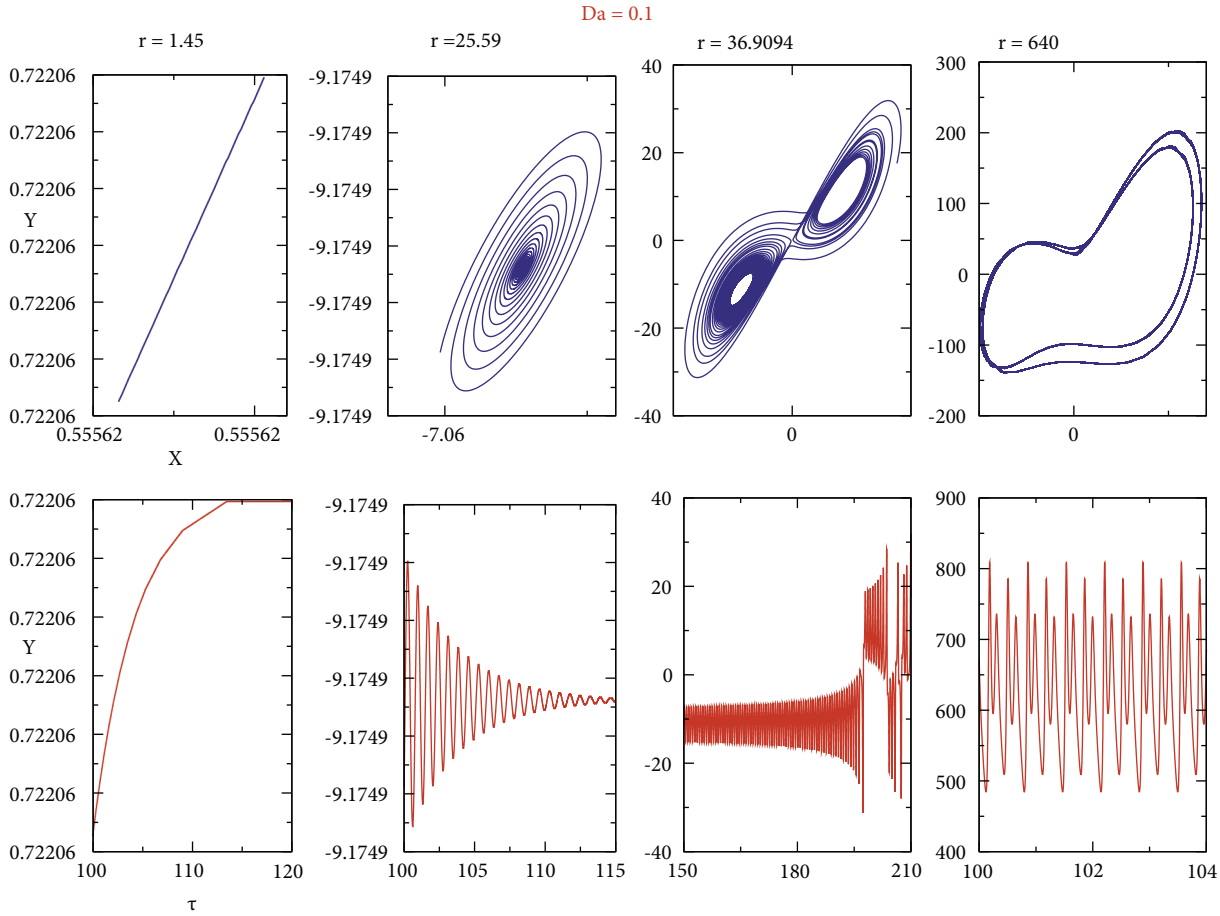

Figure 10: Phase portraits and time stories for different values of r when $Da = 0.1$, $\Lambda = 1$, $s = 0$, $Ta = 0$, $P = 10$, $k = \pi/\sqrt{2}$, $L = M_2 = 1$,$\eta = 8/3$, $\varepsilon = 1$, and $\sigma = -1/3$.

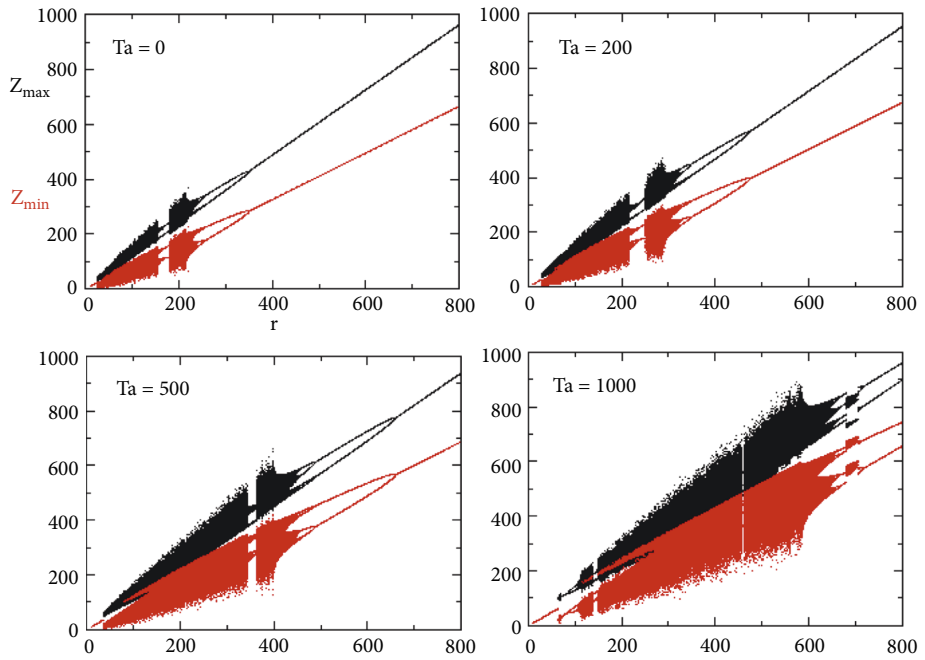

Figure 11: Diagrams of bifurcations of Z as a function of r showing the effect of the Taylor number Ta when $\Lambda = 1$, Da = 1, $s = 0$, $P = 10$, $k = \pi/\sqrt{2}$, $L = M_2 = 1$,$\eta = 8/3$, $\varepsilon = 1$, and $\sigma = -1/3$.

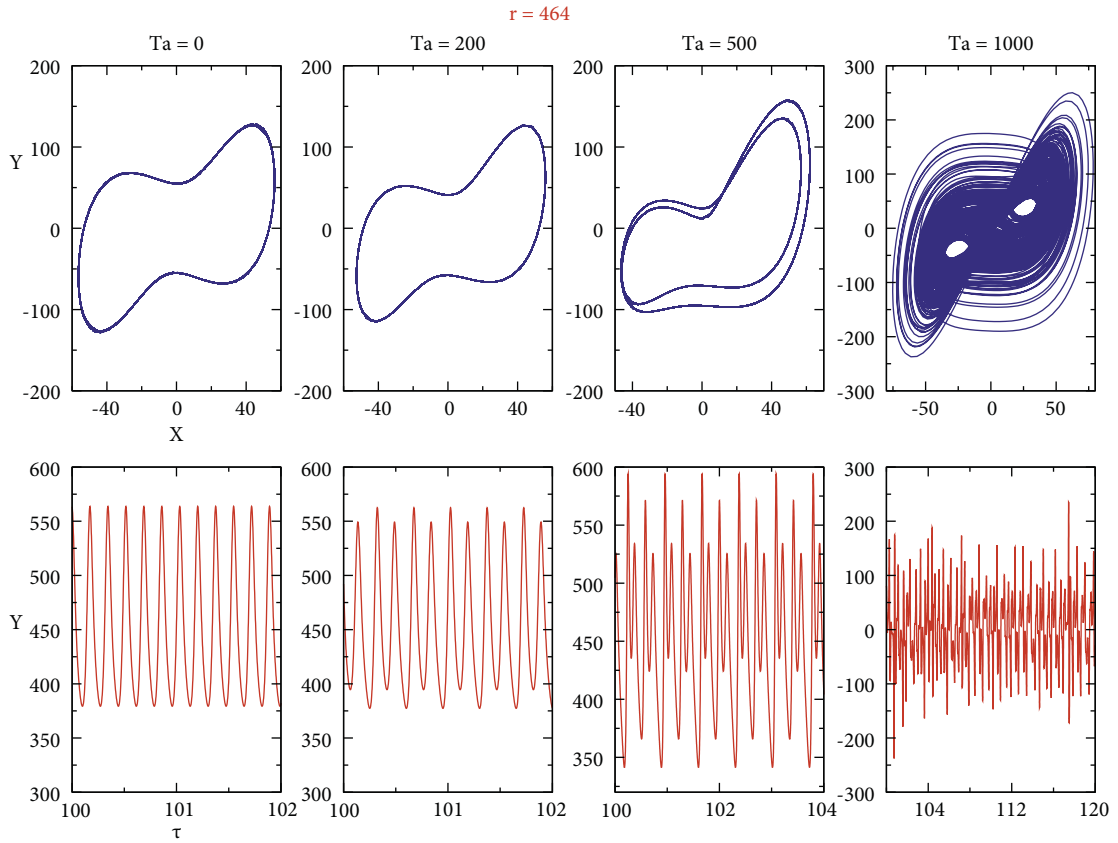

FIGURE 12: Phase portraits and time stories for a fixed reduced Rayleigh number $r = 464$ and various values of Ta for $\Lambda = 1, s = 0$, $Da = 1, P = 10$, $k = \pi/\sqrt{2}$, $L = M_2 = 1, \eta = 8/3$, $\varepsilon = 1$, and $\sigma = -1/3$.

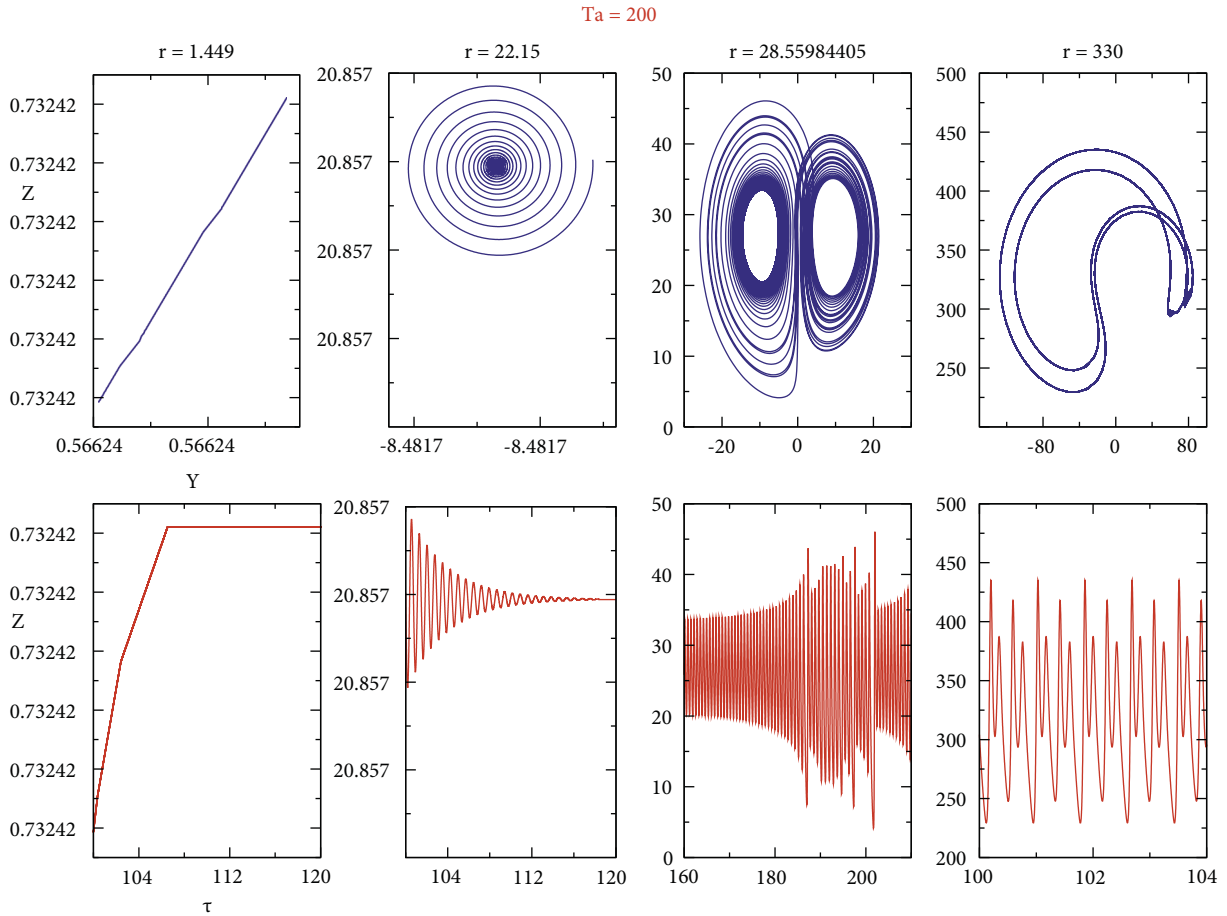

FIGURE 13: Phase portraits and time stories for various values of r when $Ta = 200$, $\Lambda = 1$, $s = 0$, $Da = 1$, $P = 10$, $L = M_2 = 1, \eta = 8/3$, $k = \pi/\sqrt{2}$, $\varepsilon = 1$, and $\sigma = -1/3$.

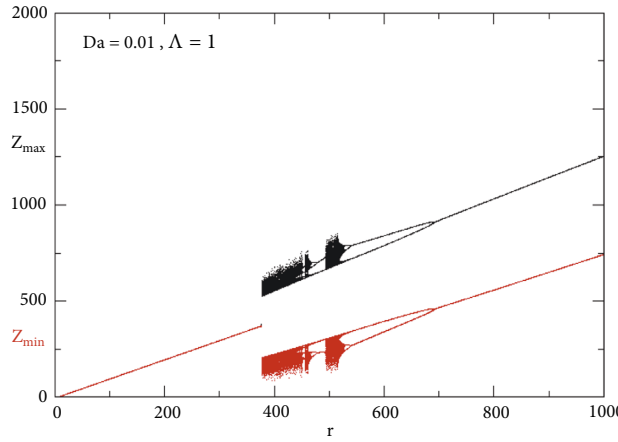

FIGURE 14: Diagrams of bifurcations of Z as a function of r representing the maxima and minima of the posttransient solution of $Z(\tau)$ for Da = 0.01Λ = 1, $s = 0$, $Ta = 0$, $k = \pi/\sqrt{2}$, $L = M_2 = 1$,$\eta = 8/3$,,$P = 10$, $\varepsilon = 1$, and $\sigma = -1/3$.

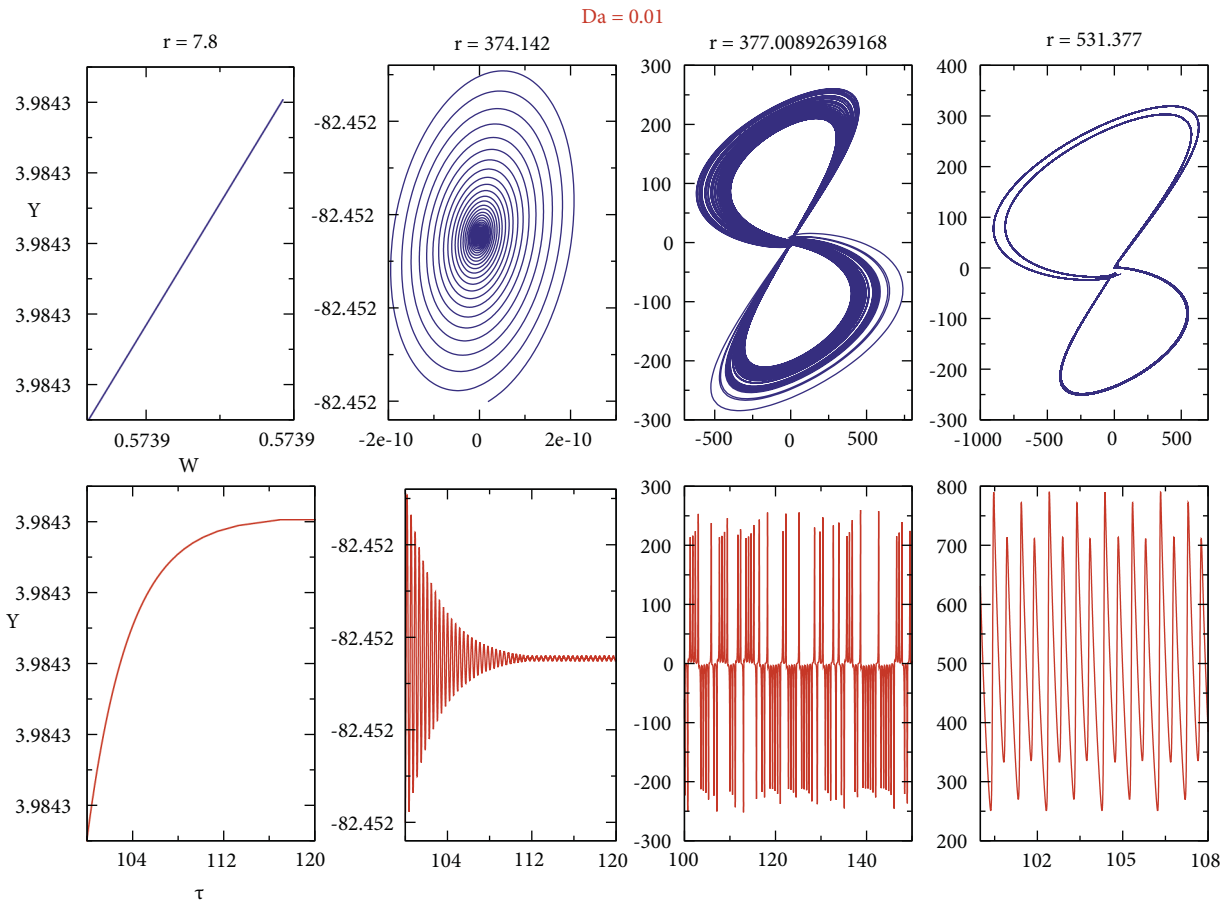

FIGURE 15: Phase portraits and time stories for various values of r when $Da = 0.01$, $\Lambda = 1$, $s = 0$, $Ta = 0, k = \pi/\sqrt{2}$, $L = M_2 = 1$,$\eta = 8/3$,$P = 10$, $\varepsilon = 1$, and $\sigma = -1/3$.

We notice that for a low value of the Darcy number Da, the system presents a surprising and advantageous behavior for the convection (Figure 14). The system is linearly stable for $r = 7.8$, oscillatory for $374.142 \le r \le 376.961$, chaotic for $377.00892639168 \le r \le 468.873$ and $494.608 \le r \le 530.147$, and then periodic for $470.098 \le r \le 492.157$ and $r \ge 531.377$ (Figure 15).

Figures 11 and 12 show that the Taylor number Ta makes the system progressively chaotic and the heat transfer gradually increases. Considering the Figure 11, for $r = 464$,

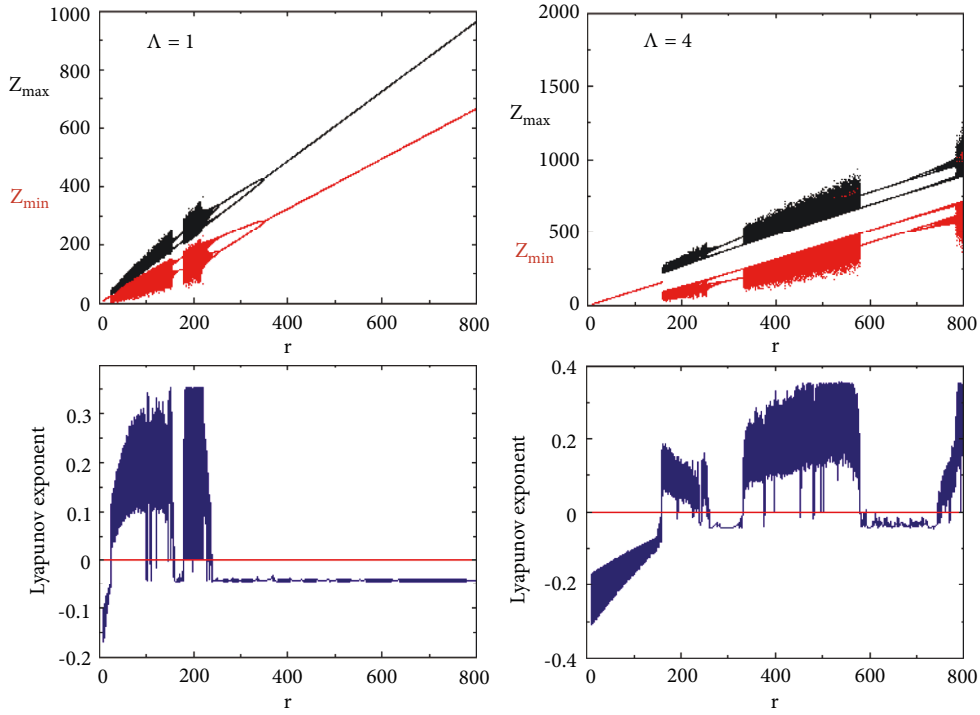

FIGURE 16: Diagrams of bifurcation and Lyapunov exponents for different values of Λ with $Da = 1$, $s = 0$, $Ta = 0$, $P = 10$, $k = \pi/\sqrt{2}$, $L = M_2 = 1$,$\eta = 8/3$, $\varepsilon = 1$, and $\sigma = -1/3$.

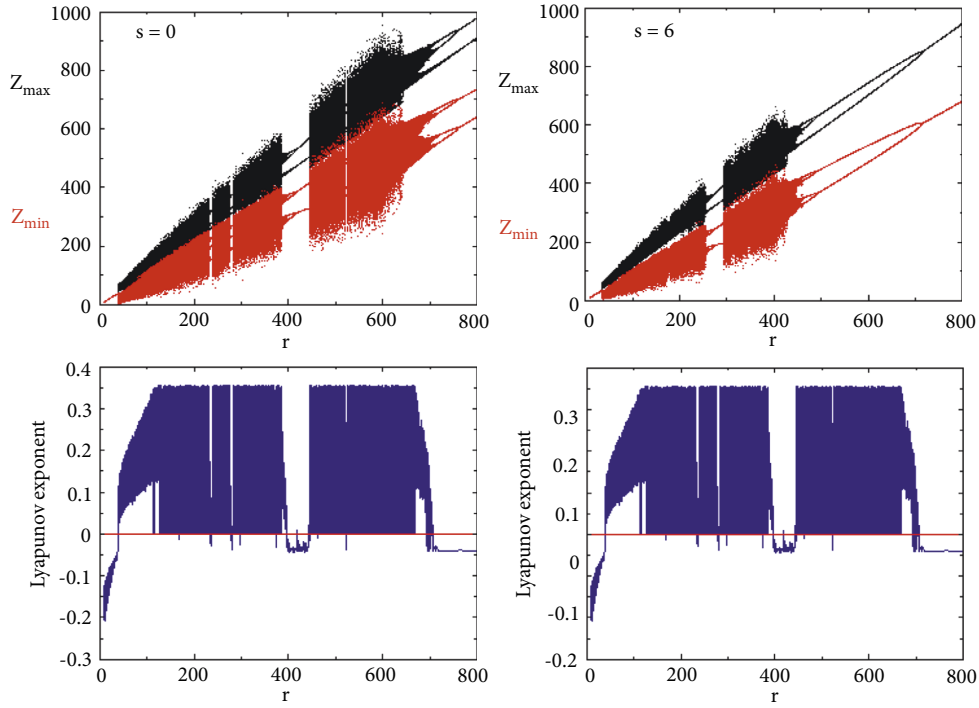

FIGURE 17: Diagrams of bifurcation and Lyapunov exponents for various values of s with Λ = 1, $Da = 0.09$, $Ta = 0$, $P = 10$, $k = \pi/\sqrt{2}$, $L = M_2 = 1$,$\eta = 8/3$, $\varepsilon = 1$, and $\sigma = -1/3$.

the system is periodic: of period 1 for Ta = 0, of period 2 for Ta = 200 then of period 4 for Ta = 500 and chaotic for Ta = 1000. The Taylor number then enlarges the chaotic domain of the system.

The system with Figure 13 is linearly stable for $r = 1.449$, oscillatory for $22.15 \le r \le 27.0973$, chaotic for $28.55984405 \le r \le 231.398$ and $252.903 \le r \le 328.823$, and then periodic for $237.85 \le r \le 250.753$ and $r \ge 330$

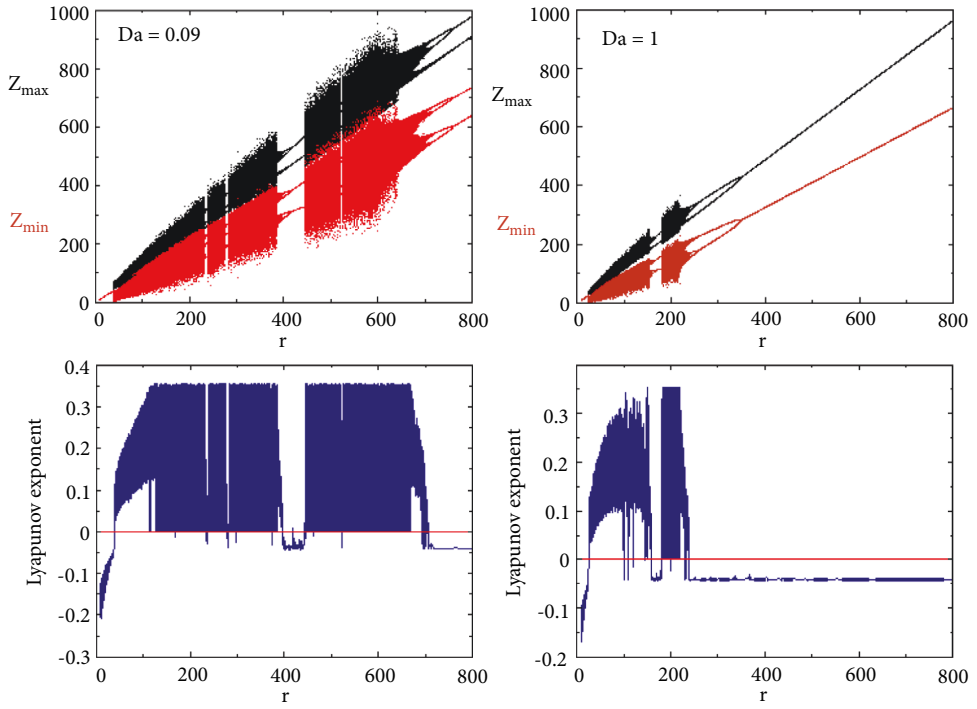

FIGURE 18: Bifurcation diagrams and Lyapunov exponents for various values of Da with $\Lambda = 1$, $s = 0$, $Ta = 0$, $P = 10$, $k = \pi/\sqrt{2}$, $L = M_2 = 1$,$\eta = 8/3$, $\varepsilon = 1$, and $\sigma = -1/3$.

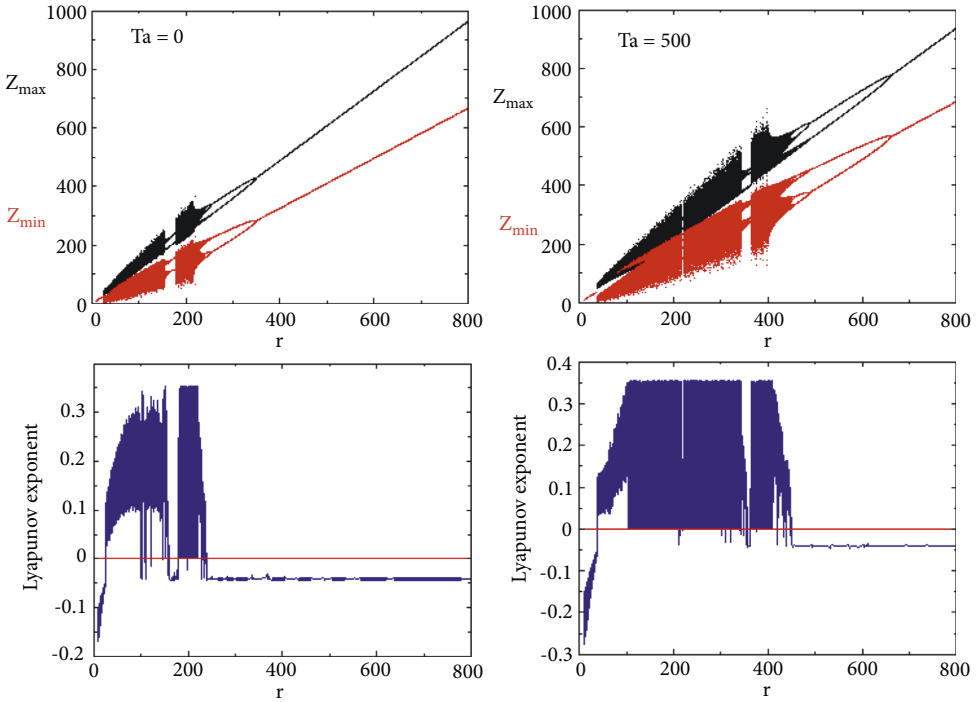

FIGURE 19: Bifurcation diagrams and its corresponding Lyapunov exponents for various values of Ta with $\Lambda = 1$, $Da = 0$, $s = 0$, $P = 10$, $k = \pi/\sqrt{2}$, $L = M_2 = 1$,$\eta = 8/3$, $\varepsilon = 1$, and $\sigma = -1/3$.

5. Conclusions

In this work, we studied the effects of the viscosity ratio Λ, the helical force intensity s, the Darcy number Da, and the Taylor number Ta on the regular and chaotic behavior of the convection in a rotating magnetic fluid in a porous medium under the helical force effect. The classical nonlinear stability theory is used. Lorenz-type model is obtained by derived from the

magnetohydrodynamics equations using the lowest Fourier modes a set of first-order ordinary differential equations.

In the absence of a magnetic field and helical in a nonrotating and a nonporous medium, the classical Lorenz model is recovered. The stability of the trivial equilibrium point has been studied with the Routh–Hurwitz criterion. The parameter regions where stationary states can occur have been identified as well as those of regular and chaotic behaviors by plotting successively bifurcation diagrams, Lyapunov exponent, and phase portraits. Throughout this study, the following results have been obtained:

(i) Increasing the ratio of viscosities Λ increases the chaotic domain, so serves to advance the heat transfer in the magnetic fluid.

(ii) Increasing the intensity s of the helical force gradually contributes to reduce the chaotic domain of the system leaving it in a periodic state. This favors the heat transfer to decrease in the fluid.

(iii) Increasing the Darcy number Da considerably reduces the domain of chaos leaving the system in a periodic state, hence serves to delay the heat transfer in the magnetic fluid.

(iv) Increasing the Taylor number Ta increases the chaotic domain, so serves to accelerate the heat transfer in the system.

We then conclude that the ratio of viscosities and the rotation enlarge the domain where chaos occurs and accelerate the heat transfer whereas the helical force and the porosity of the medium reduce the chaotic domain and delay the heat transfer. The ratio of viscosities, the porosity, the rotation, and the helical force, therefore, make it possible to control the convective chaos in the magnetic fluid.

Data Availability

No data were used to support this study.

Conflicts of Interest

The authors declare that they have no conflicts of interest.

References

[1] M. Bartuccelli, G. Gentile, and J. A. Wright, "Stable dynamics in forced systems with sufficiently high/low forcing frequency," *Chaos*, vol. 26, no. 8, Article ID 083108, 2016.

[2] H. G. Enjieu Kadji, B. R. Nana Nbendjo, J. B. Chabi Orou, and P. K. Talla, "Nonlinear dynamics of plasma oscillations modeled by an anharmonic oscillator," *Physics of Plasmas*, vol. 15, no. 3, pp. 032308–032314, 2008.

[3] H. G. Enjieu Kadji, J. B. Chabi Orou, and P. Woafo, "Regular and chaotic behaviors of plasma oscillations modeled by a modified duffing equation," *Physica Scripta*, vol. 77, no. 2, Article ID 025503, 2008.

[4] C. H. Miwadinou, L. A. Hinvi, A. V. Monwanou, and J. B. Chabi Orou, "Nonlinear dynamics of a $$\varvec{\phi}-$$ ϕ 6 - modified Duffing oscillator: resonant oscillations and transition to chaos," *Nonlinear Dynamics*, vol. 88, no. 1, pp. 97–113, 2017.

[5] T. P. Chang, "Chaotic motion in forced duffing system subject to linear and nonlinear damping," *In: Math prob eng*, vol. 12, 2017.

[6] J. J. Zebrowski, K. Grudzinski, T. Buchner et al., "Nonlinear oscillator model reproducing various phenomena in the dynamics of the conduction system of the heart," *Chaos*, vol. 17, no. 1, Article ID 015121, 2007.

[7] R. Yamapi, G. Filatrella, M. A. Aziz-Alaoui, and H. G. Enjieu Kadji, "Modeling, Stability, Synchronization, and Chaos and Their Applications to Complex Systems," *Abstract Appl Anal*, vol. 1, 2014.

[8] E. N. Lorenz, "Deterministic nonperiodic flow," *Journal of the Atmospheric Sciences*, vol. 20, no. 2, pp. 130–141, 1963.

[9] G. Sivaganesh, A. Arulgnanam, and A. N. Seethalakshmi, "A complete analytical study on the dynamics of simple chaotic systems," *Pramana - Journal of Physics*, vol. 92, no. 3, pp. 42–11, 2019.

[10] A. Singh, B. S. Bhadauria, and P. K. Gangwar, "Feedback control of chaos in porous medium under G-jitter effects," *SAMRIDDHI:A Journal of Physical Sciences, Engineering and Technology*, vol. 10, no. 1, 2018.

[11] Z. Rana, M. Aqeel, J. Ayub, and M Shaukat, "Control of chaos in thermal convection loop by state space linearization," *Chinese Journal of Physics*, vol. 58, pp. 166–178, 2019.

[12] N. Ahmed, N. A. Shah, and D. Vieru, "Natural convection with damped thermal flux in a vertical circular cylinder," *Chinese Journal of Physics*, vol. 56, no. 2, pp. 630–644, 2018.

[13] M. Izadi, M. A. Sheremet, and S. A. M. Mehryan, "Natural convection of a hybrid nanofluid affected by an inclined periodic magnetic field within a porous medium," *Chinese Journal of Physics*, vol. 65, pp. 447–458, 2020.

[14] E. Abu-Ramadan, J. M. Hay, and R. E. Khayat, "Study on the characteristics of Rayleigh-bénard convection with viscoelastic fluids," *Journal of Non-Newtonian Fluid Mechanics*, vol. 115, no. 79, 2003.

[15] L. J. Sheu, L. M. Tam, J. H. Chen, H. K. Chen, K. T. Lin, and Y. Kang, "Small and moderate Prandtl number chaotic convection in porous of feedback control," *Chaos, Solitons & Fractals*, vol. 37, pp. 113–124, 2020.

[16] M. N. Mahmud, Z. Siri, J. A. Velez, L. M. Perez, and D. Laroze, "Chaotic convection in an Oldroyd viscoelastic fluid in saturated porous medium with feedback control," *Chaos*, vol. 30, no. 7, Article ID 073109, 2020.

[17] A. Kenath, D. Soibam, and S. Khanum, "Linear and nonlinear study of Rayleigh-Bénard convection in oldroyd-B fluids under rotational modulation," *International Journal of Fluid Mechanics Research*, vol. 47, no. 5, pp. 387–397, 2020.

[18] P. Vadasz and S. Olek, "Transitions and chaos for free convection in a rotating porous layer," *International Journal of Heat and Mass Transfer*, vol. 41, no. 11, pp. 1417–1435, 1998.

[19] M. L. Hounvenou and V. Monwanou, "Chaotic convection in a magnetic fluid in rotation subjected to a pseudo-vector type force," *Physica Scripta*, vol. 97, no. 9, 13 pages, Article ID 095213, 2022.

[20] J. M. Jawdat and I. Hashim, "Low Prandtl number chaotic convection in porous media with uniform internal heat generation," *International Communications in Heat and Mass Transfer*, vol. 37, no. 6, pp. 629–636, 2010.

[21] W. Yang, X. Chen, Z. Jiang, X. Zhang, and L. Zheng, "Effect of slip boundary condition on flow and heat transfer of a double fractional Maxwell fluid," *Chinese Journal of Physics*, vol. 68, pp. 214–223, 2020.

[22] S. A. Abu-Zaid and G. Ahmadi, "Chaos in a double-diffusive convection model in the presence of noise," *Applied Mathematical Modelling*, vol. 13, no. 5, pp. 291–297, 1989.

[23] P. G. Siddheshwar and D. Radhakrishna, "Linear and nonlinear electro-convection under AC electric field," *Communications in Nonlinear Science and Numerical Simulation*, vol. 17, no. 7, pp. 2883–2895, 2012.

[24] D. Laroze, P. Siddheshwar, and H. Pleiner, "Chaotic convection in a ferrofluid," *Communications in Nonlinear Science and Numerical Simulation*, vol. 18, no. 9, pp. 2436–2447, 2013.

[25] B. S. Bhadauria, "Chaotic convection in a viscoelastic fluid saturated porous medium with a heat source," *Journal of Applied Mathematics*, vol. 2016, pp. 1–18, Article ID 1487616, 2016.

[26] L.-J. Sheu, "An autonomous system for chaotic convection in a porous medium using a thermal non-equilibrium model," *Chaos, Solitons & Fractals*, vol. 30, no. 3, pp. 672–689, 2006.

[27] L.-J. Sheu, L. M. Tam, J. H. Chen, H. K. Chen, K. T. Lin, and Y Kang, "Chaotic convection of viscoelastic fluids in porous media," *Chaos, Solitons & Fractals*, vol. 37, no. 1, pp. 113–124, 2008.

[28] V. K. Gupta, B. S. Bhadauria, I. Hasim, J. Jawdat, and A. Singh, "Chaotic convection in a rotating fluid layer," *Alexandria Engineering Journal*, vol. 54, no. 4, pp. 981–992, 2015.

[29] M. Narayana, S. N. Gaikwad, P. Sibanda, and R. B. Malge, "Double diffusive magneto-convection in viscoelastic fluids," *International Journal of Heat and Mass Transfer*, vol. 67, pp. 194–201, 2013.

[30] C. Kanchana, Yi Zhao, and P. G. Siddheshwar, "Kûppers-Lortz instability in rotating Rayleigh-Bénard convection bounded by rigid/free isothermal boundaries," *Applied Mathematics and Computation*, vol. 385, Article ID 125406, 2020.

[31] E., J. M. H. Abu-Ramadan, J. M. Hay, and R. E. Khayat, "Characterization of chaotic thermal convection of viscoelastic fluids," *Journal of Non-newtonian Fluid Mechanics*, vol. 115, no. 2-3, pp. 79–113, 2003.

[32] B. S. Bhadauria and K. Palle, "Chaotic convection in a porous under temperature modulation," *Transport in Porous Media*, vol. 107, no. 3, pp. 745–763, 2015.

[33] J. C. Umavathi and O. Anwar Beg, "Modelling the onset of thermosolutal convective instability in a non-Newtonian nanofluid-saturated porous medium layer," *Chinese Journal of Physics*, vol. 68, 2020.

[34] R. Idris and I. Hashim, "Effects of a magnetic field on chaos for low Prandtl number convection in porous media," *Nonlinear Dynamics*, vol. 62, no. 4, pp. 905–917, 2010.

[35] R. Roslan, M. N. Mahmud, and I. Hashim, "Effects of feedback control on chaotic convection in fluid-saturated porous media," *International Journal of Heat and Mass Transfer*, vol. 54, no. 1-3, pp. 404–412, 2011.

[36] M. Zhao, S. Wang, S. C. Li, Q. Y. Zhang, and U. S. Mahabaleshwar, "Chaotic Darcy-brinkman convection in a fluid saturated porous layer subjected to gravity modulation," *Results in Physics*, vol. 9, pp. 1468–1480, 2018.

[37] B. S. Bhadauria and P. Kiran, "Chaotic and oscillatory magneto-convection in a binary viscoelastic fluid under g-jitter," *International Journal of Heat and Mass Transfer*, vol. 84, pp. 610–624, 2015.

[38] P. Hounsou, A. V. Monwanou, C. H. Miwadinou, and J. B. Chabi Orou, "Effect of helical force on the stationary convection in a rotating ferrofluid," *Chinese Journal of Physics*, vol. 65, pp. 526–537, 2020.

[39] M. Kpossa and A. V. Monwanou, "'' combined effects of helical force and rotation on stationary convection of a binary ferrofluid in a porous medium," *International Journal of Applied Mechanics and Engineering*, vol. 27, no. 2, pp. 158–176, 2022.

[40] B. A. Finlayson, "Convective instability of ferromagnetic fluids," *Journal of Fluid Mechanics*, vol. 40, no. 4, pp. 753–767, 1970.

[41] F. Gantmacher, *Lectures in analytical mechanics*, Vol. 264, Mir Publishers, , Moscow, 1975.

[42] M. I. Kopp, A. V. Tur, and V. V. Yanovsky, "Chaotic Magnetoconvection in a Non-uniformly Rotating Electroconductive," *Astro-Ph.EP*, vol. 2, 2021.